Proceedings of the 2007 IEEE/RSJ International
Conference on Intelligent Robots and Systems
San Diego, CA, USA, Oct 29 - Nov 2, 2007

Enhancement of Boundary Condition Relaxation Method for 3D Hopping Motion Planning of Biped Robots

Tomomichi Sugihara and Yoshihiko Nakamura

***Abstract*— Boundary Condition Relaxation (BCR) method proposed by the authors[1] is enhanced to enable 3D hopping motion plannings from arbitrary initial conditions. The original BCR has an advantage that stepwise legged motion planning is realized in online by accepting an error from the desired goal state of the center of mass (COM) and discontinuity of the trajectory of the zero-moment point (ZMP). The main difficulty of the enhancement lies on that heterogeneous piecewise equations of motions have to be handled at once, and seamless conditioning about the angular-momentum conservation and the body attitude before/after contact phase changing have to be achieved. For the former issue, multiple boundary conditions of piecewise differential equations are set up and solved in the same way with the original BCR. They are based on an approximately mass-concentrated biped model, so that contact state transition and severe time constraints are dealt with at low computational cost. Vertical-horizontal interference of COM trajectory is also taken into account by applying numerical solution of the initial value problem of differential equations. For the latter, a Jacobian-based inverse kinematics with a continuously-varying weight-blending in accordance with the shift of the contact state is presented.**

I. INTRODUCTION

HOPPING motion can enhance the mobility of legged robots. Flight phases provide robots with three-dimensionally-expanded field of activities over the limitation of leg length, and speed up the rate of transportation. During the contact state transition, the system dynamics varies discontinuously. Particularly, the robot movement in the flight phase is ruled by the gravity and the angular momentum conservation law. For rapid hopping motion generation, the changing dynamics have to be handled with seamless switches of heterogeneous equations of motions and dynamical constraints in a short time.

Raibert et al.[2] showed that stable running can be realized by repetitive hops with a pneumatic actuator and a combination of simple maneuvers. Gregorio et al.[3] developed a tether-free monopod with a quasi-passive thruster. Hyon et al.[4] developed a dog-leg-inspired one-leg robot with a boom, and succeeded to make it run. As for studies with legged robots which are not specialized in hopping, Hirano et al.[5] proposed a cyclic jumping control of bipeds with an adaptive parameter tuning from the motion history. Also, Nagasaki et al.[6] developed a continual running pattern planning method of humanoid robots based on a spring-mass model. However, there still remain many challenges for non-continual hopping motions. Ikeda et al.[7] proposed Variable Constraint Control which computes the control input by embedding natural constraints and desired motion constraints into the equation of motion of underactuated systems, and demonstrated quadruped running. It requires accurate dynamical model of the robot, and accordingly, high computational cost. Nagasaka[8] invented a method to design humanoid motions by solving multipurpose optimization problems with partial optimization units called dynamics filter. It cannot deal with the continuity of velocity. Sugihara and Nakamura[9] proposed a contact transition control of humanoid robots based on an inverted pendulum model with virtual impedance characteristics. It is utilized by Yamamoto et al.[10] for jumping motion planning of humanoids. Tajima and Suga[11] also proposed a motion planning including flight phase of a monopod. They don't consider the angular-momentum conservation law.

Legged motion planning is the two-point-boundary-value problem with an inequality constraint on the input, where the input is the reaction force from the ground and the inequality constraint is posed since pulling forces cannot be applied at contact points. Nagasaka et al.[12] solved it in an analytical way based on an approximate dynamics, and realized biped joggings. It requires the commands throughout the motion from the beginning to the stopping, so that stepwise motion planning is not achieved. Besides, it doesn't discuss the consistency at the seams of contact phase switching. Sugihara and Nakamura[1] developed Boundary Condition Relaxation (BCR) method which enables a completely online stepwise legged motion planning by admitting some error between the desired and actually reached state. In this paper, it is enhanced to be applicable to 3D hopping motion planning from arbitrary initial condition. Four subproblems including 1) vertical COM trajectory planning for supporting phase switching, 2) horizontal COM trajectory planning under severe support-switching conditions, 3) COM trajectory modification to take vertical-horizontal interference into account, and 4) a seamless handling with angular-momentum and body attitude by weighted inverse kinematics are required to be solved for the enhancement.

II. ENHANCED BCR FOR HOPPING

A. Mass-concentrated model and EQM

The biped robot in general consists of many links and joints, so that the equation of motion takes a complex form.

This work is partially supported by Category "S" # 15100002 of Grant-in-Aid for Scientific Research, Japan Society for the Promotion of Science, and partially supported by "The Kyushu University Research Superstar Program" (president-descretionary budget).

Tomomichi Sugihara(zhidao@ieee.org) is with Graduate School of Information Science and Electrical Engineering, Kyushu University, 744, Moto'oka, Nishi-ku, Fukuoka, Japan. Yoshihiko Nakamura is with Department of Mechano-informatics, Graduate School of Information Science and Technology, University of Tokyo, 7–3–1, Hongo, Bunkyo-ku, Tokyo, Japan.

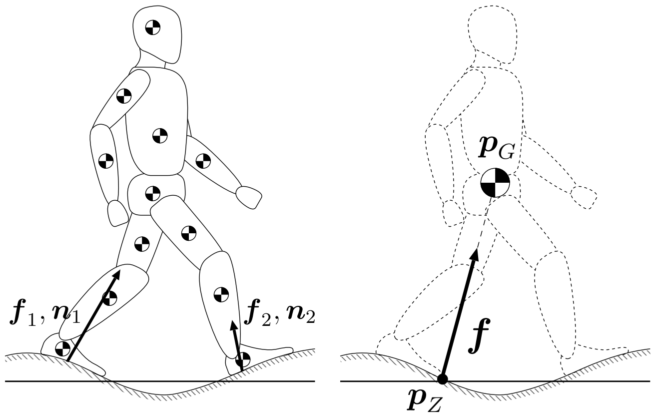

Fig. 1. Mass distributed VS mass concentrated model

By focusing on COM motion, it is simplified as follows:

$$m(\ddot{\boldsymbol{p}}+\boldsymbol{g})=\boldsymbol{f} \tag{1}$$

where m is the robot mass, $\boldsymbol{p}=[\,x\;\;y\;\;z\,]^{\mathrm{T}}$ is the COM position, $\boldsymbol{g}=[\,0\;\;0\;\;g\,]^{\mathrm{T}}$ is the gravity acceleration, and $\boldsymbol{f}=[\,f_x\;\;f_y\;\;f_z\,]^{\mathrm{T}}$ is the total linear force exerted on the robot. Let us assume that the moment about COM is small enough to be ignored in the supporting phase, and adopt the mass-concentrated model depicted as **Fig. 1**(B). Then, we get the following equation:

$$(\boldsymbol{p}-\boldsymbol{p}_Z)\times\boldsymbol{f}=\boldsymbol{0} \tag{2}$$

where $\boldsymbol{p}_Z=[\,x_Z\;\;y_Z\;\;z_Z\,]^{\mathrm{T}}$ is the ZMP[13]. Suppose the ground level z_Z is known. Since any pulling forces cannot work at any contact points, We have the following constraint condition:

$$\boldsymbol{p}_Z\in\boldsymbol{S}(t) \tag{3}$$

where $\boldsymbol{S}(t)$ is a certain convex region on the horizontal plane $z=z_Z$ and defined in accordance with the contact state between the robot and the environment. Particularly, it is the convex hull of the points in the case that all the contact points are on the same plane. In general, its form discontinuously changes as the supporting state switches.

Each component of Eq.(1) and (2) is as follows:

$$\ddot{x}=\omega^2(x-x_Z) \tag{4}$$

$$\ddot{y}=\omega^2(y-y_Z) \tag{5}$$

$$\ddot{z}=\frac{f_z}{m}-g \tag{6}$$

where

$$\omega\equiv\sqrt{\frac{\ddot{z}+g}{z-z_Z}}. \tag{7}$$

Eq.(4)(5) and (6) are regarded as differential equations of $\boldsymbol{p}$ with the inputs x_Z, y_Z and f_z. And, in the aerial phase, Eq.(1) is as follows:

$$m(\ddot{\boldsymbol{p}}+\boldsymbol{g})=\boldsymbol{0}. \tag{8}$$

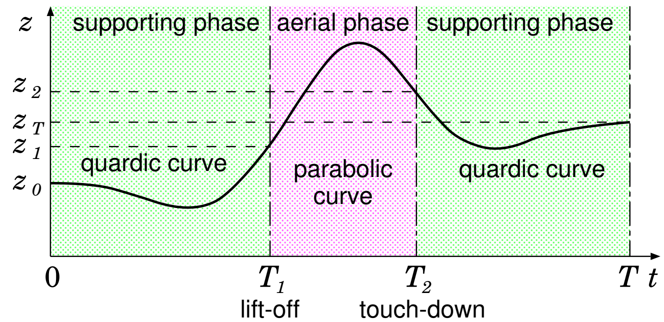

Fig. 2. Phase transition in hopping motion

The hopping motion planning is formulated as a problem in which the COM path $\boldsymbol{p}(t)$ and the corresponding input $x_Z(t)$, $y_Z(t)$ and $f_z(t)$ in $0\le t\le T$ are computed so as to connect the initial state $\boldsymbol{p}(0)=[\,x_0\;\;y_0\;\;z_0\,]^{\mathrm{T}}$, $\dot{\boldsymbol{p}}(0)=[\,v_{x0}\;\;v_{y0}\;\;v_{z0}\,]^{\mathrm{T}}$ and the goal state $\boldsymbol{p}(T)=[\,x_T\;\;y_T\;\;z_T\,]^{\mathrm{T}}$, $\dot{\boldsymbol{p}}(T)=[\,v_{xT}\;\;v_{yT}\;\;v_{zT}\,]^{\mathrm{T}}$ of the piecewise differential equation Eq.(1) and (8).

B. Vertical COM trajectory

Eq.(6) shows that the vertical COM movement is independent from the horizontal one. The vertical COM trajectory with the aerial phase in $0=t\sim T$ is segmented into three phases as **Fig. 2** shows. The first, second and third phases are from time 0 to T_1, from T_1 to T_2 and from T_1 to T, respectively.

Once the boundary conditions $z(T_1)=z_1$ and $z(T_2)=z_2$ are given, $z(t)$ in $T_1\le t\le T_2$ is determined as follows:

$$z(t)=-\frac{1}{2}g(t-T_1)(t-T_2)+\frac{z_2(t-T_1)-z_1(t-T_2)}{T_2-T_1}. \tag{9}$$

By differentiating the above with respect to time, we get:

$$\dot{z}(t)=-gt+\frac{1}{2}g(T_1+T_2)+\frac{z_2-z_1}{T_2-T_1}. \tag{10}$$

Then, the boundary condition of the velocity at T_1 and T_2 are respectively as follows:

$$\dot{z}(T_1)=v_{z1}\equiv-\frac{1}{2}g(T_1-T_2)+\frac{z_2-z_1}{T_2-T_1} \tag{11}$$

$$\dot{z}(T_2)=v_{z2}\equiv-\frac{1}{2}g(T_2-T_1)+\frac{z_2-z_1}{T_2-T_1}. \tag{12}$$

And, $\ddot{z}(t)=-g$ is satisfied at any instance. Thus, the vertical COM trajectory $z(t)$ is defined, for example, by a quartic function which satisfies $z(0)=z_0$, $\dot{z}(0)=v_{z0}$, $z(T_1)=z_1$, $\dot{z}(T_1)=v_{z1}$ and $\ddot{z}(T_1)=-g$ in $0\le t\le T_1$, and does $z(T_2)=z_2$, $\dot{z}(T_2)=v_{z2}$, $\ddot{z}(T_2)=-g$, $z(T)=z_T$ and $\dot{z}(T)=v_{zT}$ in $T_2\le t\le T$.

C. Horizontal COM trajectory

In this section, BCR is enhanced for piecewise differential equation including aerial phase. Let us assume that the effect of the vertical COM movement on the horizontal movement is sufficiently small in the supporting phase. Namely, ω in

Eq.(4) and (5) is almost a constant to be substituted for $\omega(0) = \omega_0$ in $0 \le t \le T_1$ and for $\omega(T) = \omega_T$ in $T_2 \le t \le T$, respectively. The homogeneous equations are linear, and the general solutions are obtained by finding particular solutions for designed $x_Z(t)$ and $y_Z(t)$. Since Eq.(4) and (5) are completely isomorphic, we consider only the motion in the x direction in this section.

We adopt the ZMP trajectory by the following function.

$$x_Z(t) = \begin{cases} x_{Z1} - (x_{Z1} - x_{Z0})\, e^{-\beta\omega_0 t} & (0 \le t \le T_1) \\ \text{(undefined.)} & (T_1 < t < T_2) \\ x_{ZT} - (x_{ZT} - x_{Z2})\, e^{-\beta\omega_T (t-T_2)} & (T_2 \le t \le T) \end{cases} \tag{13}$$

where β is a constant which satisfies $\beta > 0$ and $\beta \neq 1$. The choice of this function possibly creates dynamic kicking motion and discontinuous transition of support state rather easily; the larger β is chosen, the faster ZMP travels from the kicking foot to the pivotting foot. The general solution of Eq.(4) and (8) is as follows:

$$x(t) = \begin{cases} {}^1C_1 e^{\omega_0 t} + {}^1C_2 e^{-\omega_0 t} \\ \quad + \dfrac{x_{Z1} - x_{Z0}}{\beta^2 - 1} e^{-\beta\omega_0 t} + x_{Z1} & (0 \le t \le T_1) \\ x_1 + v_1 (t - T_1) & (T_1 < t < T_2) \\ {}^2C_1 e^{\omega_T (t-T_2)} + {}^2C_2 e^{-\omega_T (t-T_2)} \\ + \dfrac{x_{ZT} - x_{Z2}}{\beta^2 - 1} e^{-\beta\omega_T (t-T_2)} + x_{ZT} & (T_2 \le t \le T) \end{cases} \tag{14}$$

where ${}^1C_1$, ${}^1C_2$, x_1, v_1, ${}^2C_1$ and ${}^2C_2$ are unknown constant values. By differentiating the above, we get:

$$\dot{x}(t) = \begin{cases} \omega_0 \Big({}^1C_1 e^{\omega_0 t} - {}^1C_2 e^{-\omega_0 t} \\ \quad - \beta \dfrac{x_{Z1} - x_{Z0}}{\beta^2 - 1} e^{-\beta\omega_0 t} \Big) & (0 \le t \le T_1) \\ v_1 & (T_1 < t < T_2) \\ \omega_T \Big({}^2C_1 e^{\omega_T (t-T_2)} - {}^2C_2 e^{-\omega_T (t-T_2)} \\ - \beta \dfrac{x_{ZT} - x_{Z2}}{\beta^2 - 1} e^{-\beta\omega_T (t-T_2)} \Big) & (T_2 \le t \le T). \end{cases} \tag{15}$$

The boundary condition is expressed as follows in accordance with the continuity of position and velocity:

$$\begin{bmatrix} \boldsymbol{C}_1 & \boldsymbol{C}_2 & \boldsymbol{O} & \boldsymbol{O} \\ \boldsymbol{C}_3 & \boldsymbol{C}_4 & \boldsymbol{O} & \boldsymbol{O} \\ \boldsymbol{O} & \boldsymbol{O} & \boldsymbol{C}_1 & \boldsymbol{C}_2 \\ \boldsymbol{O} & \boldsymbol{O} & \boldsymbol{C}_5 & \boldsymbol{C}_6 \end{bmatrix} \begin{bmatrix} {}^1\boldsymbol{c} \\ {}^1\boldsymbol{x}_Z \\ {}^2\boldsymbol{c} \\ {}^2\boldsymbol{x}_Z \end{bmatrix} = \begin{bmatrix} \boldsymbol{x}_0 \\ \boldsymbol{B}_1 \boldsymbol{x}_1 \\ \boldsymbol{B}_2 \boldsymbol{x}_1 \\ \boldsymbol{x}_T \end{bmatrix} \tag{16}$$

where

$$\boldsymbol{C}_1 \equiv \begin{bmatrix} 1 & 1 \\ 1 & -1 \end{bmatrix}, \quad \boldsymbol{C}_2 \equiv \begin{bmatrix} -\gamma & \gamma + 1 \\ \beta\gamma & -\beta\gamma \end{bmatrix}$$

$$\boldsymbol{C}_3 \equiv \begin{bmatrix} \lambda_1 & \lambda_1^{-1} \\ \lambda_1 & -\lambda_1^{-1} \end{bmatrix}, \quad \boldsymbol{C}_4 \equiv \begin{bmatrix} -\gamma\lambda_1^{-\beta} & \gamma\lambda_1^{-\beta} + 1 \\ \beta\gamma\lambda_1^{-\beta} & -\beta\gamma\lambda_1^{-\beta} \end{bmatrix}$$

$$\boldsymbol{C}_5 \equiv \begin{bmatrix} \lambda_2 & \lambda_2^{-1} \\ \lambda_2 & -\lambda_2^{-1} \end{bmatrix}, \quad \boldsymbol{C}_6 \equiv \begin{bmatrix} -\gamma\lambda_2^{-\beta} & \gamma\lambda_2^{-\beta} + 1 \\ \beta\gamma\lambda_2^{-\beta} & -\beta\gamma\lambda_2^{-\beta} \end{bmatrix}$$

$$\boldsymbol{B}_1 \equiv \begin{bmatrix} 1 & 0 \\ 0 & \omega_0^{-1} \end{bmatrix}, \quad \boldsymbol{B}_2 \equiv \begin{bmatrix} 1 & T_2 - T_1 \\ 0 & \omega_T^{-1} \end{bmatrix}$$

$$\gamma \equiv \frac{1}{\beta^2 - 1}, \quad \lambda_1 \equiv e^{\omega_0 T_1}, \quad \lambda_2 \equiv e^{\omega_T (T - T_2)}$$

$${}^1\boldsymbol{c} \equiv \begin{bmatrix} {}^1C_1 \\ {}^1C_2 \end{bmatrix}, {}^2\boldsymbol{c} \equiv \begin{bmatrix} {}^2C_1 \\ {}^2C_2 \end{bmatrix}, {}^1\boldsymbol{x}_Z \equiv \begin{bmatrix} x_{Z0} \\ x_{Z1} \end{bmatrix}, {}^2\boldsymbol{x}_Z \equiv \begin{bmatrix} x_{Z2} \\ x_{ZT} \end{bmatrix}$$

$$\boldsymbol{x}_0 \equiv \begin{bmatrix} x_0 \\ v_{x0}/\omega_0 \end{bmatrix}, \quad \boldsymbol{x}_1 \equiv \begin{bmatrix} x_1 \\ v_1 \end{bmatrix}, \quad \boldsymbol{x}_T \equiv \begin{bmatrix} x_T \\ v_{xT}/\omega_T \end{bmatrix}.$$

The coefficient matrix of the left side is regular; once given $\boldsymbol{x}_0$, $\boldsymbol{x}_T$ and $\boldsymbol{x}_1$, the ZMP trajectory, and accordingly, the COM trajectory are uniquely defined from Eq.(16), which do not necessarily satisfy Eq.(3). Let us reconsider the properties of each unknown in Eq.(16). First, $\boldsymbol{x}_0$ must be satisfied for the motion continuity, while $\boldsymbol{x}_T$ can accept a certain amount of error from the desired ${}^d\boldsymbol{x}_T$. ${}^1\boldsymbol{x}_Z$ and ${}^2\boldsymbol{x}_Z$ should be in the neighborhood of ${}^{d1}\boldsymbol{x}_Z$ and ${}^{d2}\boldsymbol{x}_Z$, respectively, which are consistent with the planned foot placement in order to satisfy Eq.(3). In particular, x_{Z1} and x_{Z2} are the ZMP immediately before lift-off and after landing, respectively, so that the acceptable error level is small, while $\boldsymbol{x}_1$, ${}^1\boldsymbol{c}$ and ${}^2\boldsymbol{c}$ can be arbitrary values. Based on these facts, let us rewrite Eq.(16) as follows:

$$\tilde{\boldsymbol{C}}\boldsymbol{\eta} = \boldsymbol{\chi} + \tilde{\boldsymbol{x}}_T \quad \Longleftrightarrow \quad \boldsymbol{\eta} = \tilde{\boldsymbol{C}}^{-1}(\boldsymbol{\chi} + \tilde{\boldsymbol{x}}_T) \tag{17}$$

where

$$\tilde{\boldsymbol{C}} \equiv \begin{bmatrix} 1 & 1 & -\gamma & 0 & 0 & 0 & 0 & 0 \\ 1 & -1 & \beta\gamma & 0 & 0 & 0 & 0 & 0 \\ \lambda_1 & \lambda_1^{-1} & -\gamma\lambda_1^{-\beta} & -1 & 0 & 0 & 0 & 0 \\ \lambda_1 & -\lambda_1^{-1} & \beta\gamma\lambda_1^{-\beta} & 0 & -\omega_0^{-1} & 0 & 0 & 0 \\ 0 & 0 & 0 & -1 & -(T_2 - T_1) & 1 & 1 & \gamma + 1 \\ 0 & 0 & 0 & 0 & -\omega_T^{-1} & 1 & -1 & -\beta\gamma \\ 0 & 0 & 0 & 0 & 0 & \lambda_2 & \lambda_2^{-1} & \gamma\lambda_2^{-\beta} + 1 \\ 0 & 0 & 0 & 0 & 0 & \lambda_2 & -\lambda_2^{-1} & -\beta\gamma\lambda_2^{-\beta} \end{bmatrix}$$

$$\boldsymbol{\eta} \equiv \begin{bmatrix} {}^1C_1 \\ {}^1C_2 \\ x_{Z0} \\ x_1 \\ v_1 \\ {}^2C_1 \\ {}^2C_2 \\ x_{ZT} \end{bmatrix}, \; \boldsymbol{\chi} \equiv \begin{bmatrix} x_0 - (\gamma + 1)\,{}^d x_{Z1} \\ \dfrac{v_0}{\omega_0} + \beta\gamma\,{}^d x_{Z1} \\ -(\gamma\lambda_1^{-\beta} + 1)\,{}^d x_{Z1} \\ \beta\gamma\lambda_1^{-\beta}\,{}^d x_{Z1} \\ \gamma\,{}^d x_{Z2} \\ -\beta\gamma\,{}^d x_{Z2} \\ \gamma\lambda_2^{-\beta}\,{}^d x_{Z2} \\ -\beta\gamma\lambda_2^{-\beta}\,{}^d x_{Z2} \end{bmatrix}, \; \tilde{\boldsymbol{x}}_T \equiv \begin{bmatrix} \boldsymbol{0} \\ \boldsymbol{x}_T \end{bmatrix}.$$

By abstracting the rows about x_{Z0} and x_{ZT} from Eq.(17), we get:

$$\begin{bmatrix} x_{Z0} \\ x_{ZT} \end{bmatrix} = \boldsymbol{D}_1 \boldsymbol{\chi} + \boldsymbol{D}_2 \boldsymbol{x}_T. \tag{18}$$

Then, let us set the following quadratic programming problem:

$$\frac{1}{2}(\boldsymbol{\xi} - {}^d\boldsymbol{\xi})^{\mathrm{T}} \boldsymbol{Q}^{-1} (\boldsymbol{\xi} - {}^d\boldsymbol{\xi}) \longrightarrow \textit{minimum} \quad \text{subject to} \quad \boldsymbol{D}\boldsymbol{\xi} = \boldsymbol{s} \tag{QP}$$

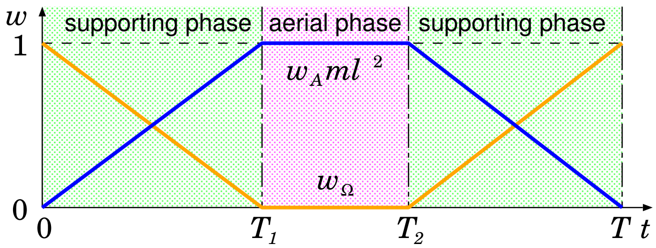

Fig. 3. Variable weight in accordance with contact phase

where

$$\begin{aligned}
&\boldsymbol{\xi} \equiv \left[x_{Z0} \quad x_{ZT} \quad x_T \quad v_T/\omega_T\right]^{\mathrm{T}} \\
&{}^d\boldsymbol{\xi} \equiv \left[{}^dx_{Z0} \quad {}^dx_{ZT} \quad {}^dx_T \quad {}^dv_T/\omega_T\right]^{\mathrm{T}} \\
&\boldsymbol{Q} \equiv \mathrm{diag}\{q_i\} \qquad (i = 1 \sim 4,\ q_i > 0) \\
&\boldsymbol{D} \equiv \left[\boldsymbol{1} \quad -\boldsymbol{D}_2\right], \quad \boldsymbol{s} \equiv \boldsymbol{D}_1\boldsymbol{\chi}.
\end{aligned}$$

Solving the problem (QP), we get:

$$\boldsymbol{\xi} = {}^d\boldsymbol{\xi} - \boldsymbol{Q}\boldsymbol{D}^T(\boldsymbol{D}\boldsymbol{Q}\boldsymbol{D}^T)^{-1}(\boldsymbol{D}{}^d\boldsymbol{\xi} - \boldsymbol{s}). \tag{19}$$

${}^1\boldsymbol{c}$, ${}^2\boldsymbol{c}$ and $\boldsymbol{x}_1$ are obtained from Eq.(17). Eq.(3) is satisfied by setting ${}^dx_{Z0}$ and ${}^dx_{ZT}$ inside of the supporting region at $t = 0$ and $t = T$, respectively, and choosing sufficiently large q_1 and q_2. The foot trajectories are designed so as to be consistent with the planned $x_z(t)$ and the moment of lift-off T_1 and landing T_2.

D. Absorption of vertical-horizontal interference of COM trajectory

In the previous subsection, ω was supposed to be a constant in each time segment. In cases of hopping, the locus of ZMP deviates from the planned trajectory as the COM makes large vertical movements in a short time. In order to satisfy the condition (3) at any moment, ZMP tracking should be prioritized over COM tracking in a short span. Now, we have the ZMP trajectory $x_Z(t)$ and the vertical COM trajectory $z(t)$ as functions of time, By putting them into Eq.(4) and (8), they become differential equations with time-dependent forcing terms, so that they can be solved as the initial value problems. And, the horizontal COM trajectory which matches the ZMP trajectory is computed by numerical approaches such as Runge-Kutta-Gill's method.

III. IK WITH VARYING WEIGHT FOR ATTITUDE/ ANGULAR-MOMENTUM CONSTRAINTS

In this section, an inverse kinematics algorithm is presented to achieve the planned COM and foot trajectories, to balance trunk attitude control in the supporting phase and to ensure the angular-momentum conservation in the aerial phase.

Suppose the generalized coordinates of the robot including 6DOF of the floating-baselink is $\boldsymbol{\theta}$. A small deviation of position and orientation of COM and extremities $\Delta\boldsymbol{p}_U$ is related to a small deviation of $\boldsymbol{\theta}$, $\Delta\boldsymbol{\theta}$ by the Jacobian matrix $\boldsymbol{J}_U$[14] as follows.

$$\Delta\boldsymbol{p}_U = \boldsymbol{J}_U\Delta\boldsymbol{\theta} \tag{20}$$

In the supporting phase, the following constraint is validated in order to let the trunk attitude track the planned path:

$$\boldsymbol{J}_{\Omega 0}\Delta\boldsymbol{\theta} = \Delta\boldsymbol{\Omega}_0 \tag{21}$$

where $\boldsymbol{J}_{\Omega 0}$ is the Jacobian matrix about the attitude deviation of the trunk link, and $\Delta\boldsymbol{\Omega}_0$ is the error vector between the desired and the current trunk attitude. On the other hand, the robot behavior is ruled by the angular-momentum conservation law in the aerial phase. Namely, the following equation must be satisfied in any $t = T_1 \sim T_2$:

$$\boldsymbol{J}_A\Delta\boldsymbol{\theta} = {}^d\boldsymbol{L} \tag{22}$$

where ${}^d\boldsymbol{L}$ is the desired angular-momentum about COM in the aerial phase, and $\boldsymbol{J}_A$ is defined as follows:

$$\boldsymbol{J}_A \equiv \sum_{i=1}^{N}\left\{m_i[(\boldsymbol{p}_i - \boldsymbol{p})\times]\boldsymbol{J}_{Gi} + \boldsymbol{R}_i{}^i\boldsymbol{I}_i{}^i\boldsymbol{J}_{\Omega i}\right\}. \tag{23}$$

N is the number of links, m_i is the mass of i'th link, $\boldsymbol{p}_i$ is the COM of i'th link, $\boldsymbol{J}_{Gi}$ is the Jacobian matrix about COM displacement of i'th link, $\boldsymbol{R}_i$ is the attitude matrix of i'th link, ${}^i\boldsymbol{I}_i$ is the inertia tensor about COM of i'th link with respect to the link local frame Σ_i, ${}^i\boldsymbol{J}_{\Omega i}$ is the Jacobian matrix about the attitude deviation of i'th link with respect to Σ_i, and $[*\times]$ means the skew-symmetric outer-product matrix.

In order to make the constraint shift from (21) to (22) seamlessly at the transition of contact state, we impose both conditions at any moment with continuously varying weights as **Fig. 3** depicts. The weights $w_{\Omega 0}$ for (21), and w_A for (22), respectively, are given as follows:

$$w_{\Omega 0} = \begin{cases} \dfrac{T_1 - t}{T_1} & (0 \le t \le T_1) \\ 0 & (T_1 \le t \le T_2) \\ \dfrac{t - T_2}{T - T_2} & (T_2 \le t \le T) \end{cases} \tag{24}$$

$$w_A = \frac{1}{ml^2}\begin{cases} \dfrac{t}{T_1} & (0 \le t \le T_1) \\ 1 & (T_1 \le t \le T_2) \\ \dfrac{T - t}{T - T_2} & (T_2 \le t \le T) \end{cases} \tag{25}$$

where l is a characteristic length of the robot, its height for instance. The latter w_A is divided by ml^2 for absorption of physically different natures of each constraint. For the same purpose, the weight on (20) is also divided by l. By applying Newton=Raphson's method and the singularity-robust inverse matrix[15], these weighted constraints are resolved into the whole joint motion. It is known that the singularity-robust motion rate resolution yields numerical error and thus causes dissatisfaction of strict physical and kinematic consistency particularly about the angular-momentum conservation and foot-contact state. However, we prioritized numerical robustness against over-constrained (and consequently ill-conditioned) inverse kinematics. And, we experimentally verified that it does not lead to serious problem for the achievement of the desired motions.

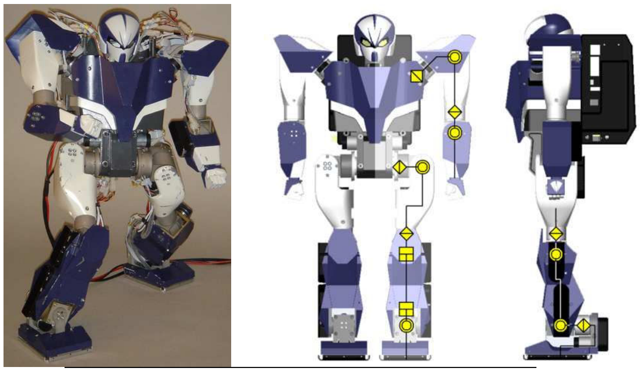

Name:	UT-μ2:magnum
height:	540 [mm]
weight:	7.5 [kg]
Number of joints:	20 (4 for each arm, 6 for each leg)

Fig. 4. External view and specifications of the robot

IV. EXAMPLE

This section shows an example forward-hopping motion generated by the proposed method using a humanoid robot UT-μ2 in Fig.4. When it stands upright, the height of COM is about 0.3[m]. The initial positions of left-foot, right-foot and COM are $[\, 0 \;\; -0.0485 \;\; 0 \,]^{\mathrm{T}}$, $[\, 0 \;\; 0.0485 \;\; 0 \,]^{\mathrm{T}}$ and $[\, 0 \;\; 0 \;\; 0.26 \,]^{\mathrm{T}}$, respectively. The robot was initially in the stationary state. The commanded parameters for the motion were $T_1 = 0.2$, $T_2 = 0.3$, $T = 0.5$, $z_1 = 0.27$, $z_2 = 0.28$, $z_T = 0.27$, $x_{Z0} = 0$, $x_{Z1} = 0$, $x_{Z2} = 0.05$, $x_{Z3} = 0.05$, $\beta = 1.5$, ${}^{d}x_T = 0.05$, the desired angular-momentum in the aerial phase ${}^{d}\boldsymbol{L} = \boldsymbol{0}$, the lift height of the feet $h_K = 0.02$, and the weighting matrix for (QP) $\boldsymbol{Q} = \mathrm{diag}\{1, 2, 0.2, 0.1\}$. The planned trajectories are plotted in **Fig. 6**(A)∼(C); (A) for COM, the feet and ZMP along x-axis, (B) for COM and the feet along z-axis, and (C) for the vertical acceleration of COM. We applied Runge-Kutta-Gill's method for horizontal COM trajectory modification. A particular difference caused by the modification in the forward COM velocity at the lift-off is seen in (A). In this example, the error of COM position from the desired one along x-axis at the end is within 8[mm].

Fig. 6(D) shows the ZMP locus of inverse dynamics analysis for the planned motion. The hatched area in the figure represents $\boldsymbol{S}(t)$. Comparing with (C), one can find that the gap of ZMP from the planned trajectory grows as the vertical COM acceleration decreases, particularly around the moment of lift-off and landing. In those terms, however, it is thought that the magnitude of the ground reaction force is not so large that the tipping moment acting against the robot is seriously large. (E) shows the pitch angle of the trunk attitude. Although the referential angle was always 0, the actual angle automatically varied due to the continuously changing weights of constraints, which is compatible with the angular-momentum conservation. **Fig. 5** is a series of snapshots of the examined hopping motion.

The above computation ran on a PC which is equipped with CPU:Intel Pentium M 1GHz and RAM:256MB. The inverse kinematics required about 0.007[s] for each step.

V. CONCLUSION

This paper enhanced the Boundary Condition Relaxation method proposed by the authors to 3D hopping motion planning of biped robots from arbitrary initial conditions. As well as the original BCR method, a stepwise hopping motion planning can be achieved. It features the following four properties.

i) Vertical COM trajectory which satisfies the desired lift-off/landing time and the height of COM at those instances is planned.
ii) Horizontal trajectories of both COM and ZMP which satisfies severe time constraints derived from the above vertical motion under the inequality constraint about the external reaction force are simultaneously computed. Multiple boundary conditions of heterogeneous piecewise equations of motions are set up and solved in the same way with the original BCR.
iii) Since it computes ZMP trajectory in the above process, the interference between vertical and horizontal movements can be taken into account by modifying the horizontal COM trajectory.
iv) Seamless shift of the constraints from the attitude control condition to the angular-momentum conservation condition at the transition of contact state is achieved by singularity-robust inverse kinematics with continuously varying weights.

REFERENCES

[1] T. Sugihara and Y. Nakamura, "A Fast Online Gait Planning with Boundary Condition Relaxation for Humanoid Robots," in *Proceedings of the 2005 IEEE International Conference on Robotics & Automation*, 2005, pp. 306–311.

[2] M. H. Raibert, H. B. B. Jr., and M. Chepponis, "Experiments in Balance with a 3D One-Legged Hopping Machine," *The International Journal of Robotics Research*, vol. 3, no. 2, pp. 75–92, 1984.

[3] P. Gregorio, M. Ahmadi, and M. Buehler, "Design, Control, and Energetics of an Electrically Actuated Legged Robot," *IEEE Transaction of Systems, Man, and Cybernetics*, vol. 27B, no. 4, pp. 626–634, 1997.

[4] S. H. Hyon and T. Mita, "Development of a Biologically Inspired Hopping Robot – "Kenken"," in *Proceedings of the 2002 IEEE International Conference on Robotics & Automation*, 2002, pp. 3984–3991.

[5] T. Hirano, T. Sueyoshi, and A. Kawamura, "Development of ROCOS (Robot Control Simulator) - Jump of human-type biped root by the adaptive impedance control," in *Proceeding of 6th International Workshop on Advanced Motion Control*, 2000.

[6] T. Nagasaki, S. Kajita, K. Yokoi, K. Kaneko, and K. Tanie, "Running Pattern Generation and Its Evaluation Using a Realistic Humanoid Model," in *Proceedings of the 2003 IEEE International Conference on Robotics & Automation*, 2003, pp. 1336–1342.

[7] T. Mita and T. Ikeda, "Proposal of a Variable Constraint Control for SMS and Its Application to Running and Jumping Quadruped," in *IEEE Internatinal Conference on System, Man and Cybernetics*, 1999.

[8] K. Nagasaka, "The Whole Body Motion Generation of Humanoid Robot Using Dynamics Filter(in Japanese)," Ph.D. dissertation, University of Tokyo, 2000.

[9] T. Sugihara and Y. Nakamura, "Contact Phase Invariant Control for Humanoid Robot based on Variable Impedant Inverted Pendulum Model," in *Proceedings of the 2003 IEEE International Conference on Robotics & Automation*, 2003, pp. 51–56.

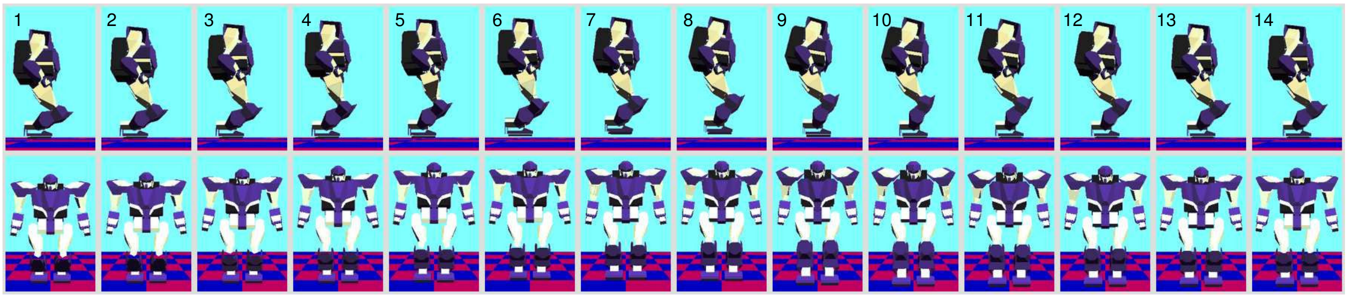

Fig. 5. A hopping-forward motion by a miniature humanoid robot

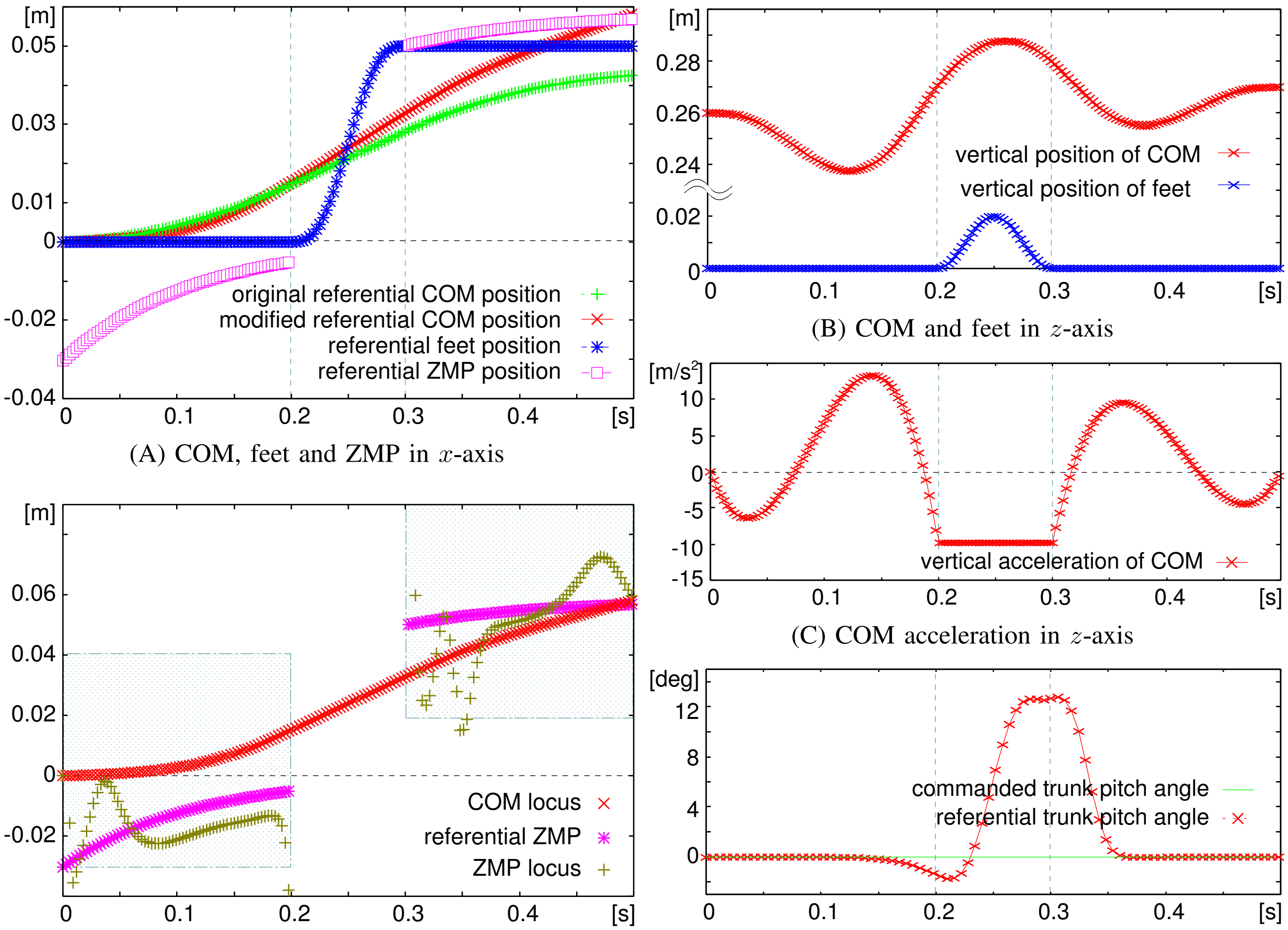

(A) COM, feet and ZMP in x-axis

(B) COM and feet in z-axis

(C) COM acceleration in z-axis

(D) ZMP locus by inverse dynamics

(E) pitch angle of trunk

Fig. 6. Planned trajectory of COM, foot and ZMP

[10] K. Yamamoto, T. Sugihara, and Y. Nakamura, "Legged Motion Planning of Humanoid Robots That Change Contact States Variedly under Severe Time Constraints (in Japanese)," in *Proceedings of the 12th Japanese Concil of International Federation for the Theory of Machines and Mechanisms Symposium*, 2006, pp. 43–46.

[11] R. Tajima and K. Suga, "Motion having a Flight Phase: Experiments Involving a One-legged Robot," in *Proceedings of the 2006 IEEE International Conference on Intelligent Robots and Systems*, 2006, pp. 1726–1731.

[12] K. Nagasaka, Y. Kuroki, S. Suzuki, Y. Itoh, and J. Yamaguchi, "Integrated Motion Control for Walking, Jumping and Running on a Small Bipedal Entertainment Robot," in *Proceedings of the 2004 IEEE International Conference on Robotics and Automation*, 2004, pp. 3189–3914.

[13] M. Vukobratović and J. Stepanenko, "On the Stability of Anthropomorphic Systems," *Mathematical Biosciences*, vol. 15, no. 1, pp. 1–37, 1972.

[14] D. E. Whitney, "The Mathematics of Coordinated Control of Prosthetic Arms and Manipulators," *Transactions of the ASME, Journal of Dynamic Systems, Measurement, and Control*, vol. 94, no. 4, pp. 303–309, 1972.

[15] Y. Nakamura and H. Hanafusa, "Inverse Kinematic Solutions with Singularity Robustness for Robot Manipulator Control," *Journal of Dynamic Systems, Measurement and Control*, vol. 108, pp. 163–171, 1986.